Reverse Engineering of Micro Turbojet Centrifugal Compressor Design Based on Parametric CAD Data

<Tamer S. Fathy>[1], <Aly M. Elzahaby>[2], <Mohamed K. Khalil>[3]

[1] Corresponding author is currently pursuing PhD degree program in Military Technical College (MTC), Egypt,
tamer_vivi01@yahoo.com

[2] Professor, Depart of Mechanical Power Engineering, Tanta University, Tanta, Egypt,
elzahaby47@gmail.com

[3] Doctor, Military Technical College (MTC), Cairo, Egypt,
khilo99@yahoo.com.

Abstract: ***Engineering is the profession involved in designing, manufacturing, constructing, and maintaining of products, systems, and structures. It can be divided into two branches, forward and reverse engineering. Forward engineering is the traditional approach in which a design process is performed from the requirements stage up to physical implementation of a product. In some situations, there may be a physical part without any technical details, such as drawings, bills of material, or without engineering data, such as thermal and electrical properties. The process of duplicating an existing component, subassembly, or product, without the aid of drawings, documentation, or computer model is known as reverse engineering [1], [2]. Reverse engineering is also described as the process of obtaining a geometric computer-aided design (CAD) model from 3-D points acquired by scanning and digitizing of existing parts.***

The engine used in this study is JetCat P200-SX, which is a single spool turbojet. It is comprised of a standard inlet, a single stage centrifugal compressor with vane diffusers, an annular combustor, a single stage axial turbine and convergent nozzle. The JetCat P200-SX turbojet engine complete technical specifications are given in Table 1.

The part geometry is first obtained with the help of scanning technology. Then with the use of Siemens NX software, the three-dimensional image of a centrifugal compressor is obtained.

This paper concerns with application of reverse engineering in obtaining the geometry of centrifugal compressor by using a design methodology (written in MATLAB) collected and approved by Dr. Aly Elzahaby at Military Technical College (MTC) and finally comparing the obtained results with CFD simulation at design point.

Keywords: Reverse Engineering; Laser Scanning; CMM; MATLAB; Micro turbojet.

1. Introduction

In aerospace field, two primary types of compressors exist: axial and centrifugal. This paper focuses on the centrifugal compressor, which is used mainly in small and micro gas turbine engines as it significantly reduces the complexity and overall length of the engine.

The objective of the compressor is to increase the pressure of the flow before it goes into the combustor. If higher pressure can be achieved, the greater the overall performance of the engine. The main components of a turbojet engine can be illustrated using figure 1.

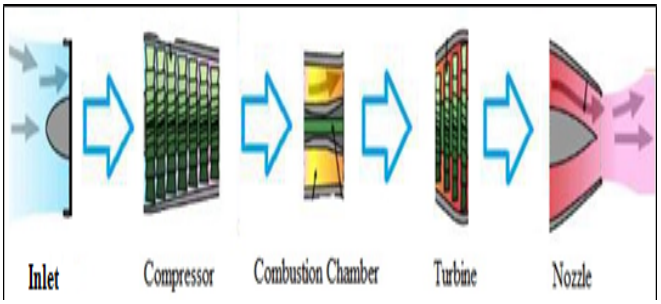

Figure 1: Components of a typical turbojet engine

Table 1: JetCat P200-SX Technical Specifications as Provided from Manufacture [3]

Compressor pressure ratio, π_{ct}	3.7
Idle thrust	9 N
Maximum Thrust, *F*	230 N
Idle Speed	33,000 rpm
Maximum Speed	112,000 rpm
Maximum Exhaust Gas Temperature (EGT)	750℃
Mass Flow Rate, $\dot{m}$	0.45 kg/s
Maximum exhaust velocity	1,840 km/h
Maximum fuel consumption	0.584 kg/min (0.1523 kg_f/N.h)
Fuel mixture (By volume)	95% Jet-A1+ 5% Mobil jet oil
	254

The JetCat P200-SX centrifugal compressor is composed of several parts including, impeller, vaneless diffuser, vanned diffusers (radial and axial) and outlet elbow as seen in figure 2. Each of these parts has to be separately modelled independently and then assembled together to form the whole compressor geometry. The impeller is composed of 6 main blades and 6 splitters (secondary blades) to reduce the blockage of the flow and the radial vanned diffuser contains 17 radial blades, while the axial one contains 34 guide vanes.

Centrifugal compressors can be broken into two main components: the impeller and diffusers. The impeller increases the flow velocity and pressure with changing the flow direction from axial to radial. The diffusers then slow the flow down to increase the pressure going into the combustor, which allows for high efficiency combustion process.

Reverse engineering can be used due to the following reasons [4]:

- Gathering required technical information about a part which has unknown geometrical and performance specifications,
- Inspection and quality control,
- Manufacturing of a part for which there are no CAD data,
- Exploring new avenues to improve product performance.

The main objectives of this work can be summarized as follows:

- Disassembling the engine to reach the centrifugal compressor which needs to be redesigned.
- Scanning the compressor to get the point cloud. The scanning can be done using a coordinate measuring machine (CMM) or a 3-D optical scanning scanner according to reverse engineering requirements.
- Processing the points cloud includes merging of points cloud if the part is scanned in several settings. If too many points are collected, then sampling of the points should be possible.
- To create the polygon model and prepare *stl* type files.
- To prepare the surface model to be sent to Siemens NX program for analysis and to create the 3D model.

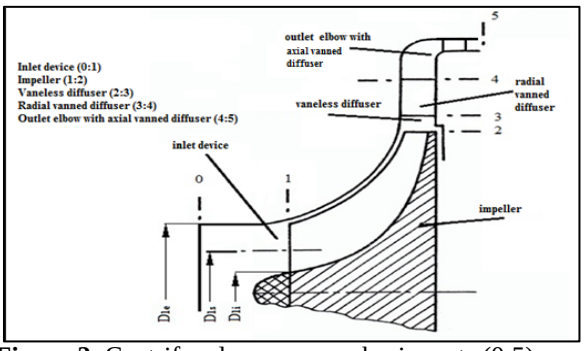

Figure 2: Centrifugal compressor basic parts (0:5)

2. Compressor Geometry Model

The original geometry of the JetCat P200-SX centrifugal compressor impeller is complex and 3D twisted as in figure 3, to obtain the full geometry of the impeller and the other parts of the compressor, a reverse engineering methodology is followed. In the beginning the turbojet engine is carefully disassembled until the centrifugal compressor is clearly observed. Then by using CMM and optical scanning on the engine, a 3D model of the compressor is gathered. Then, the model is processed on Siemens NX software to handle the parameterized model of the compressor impeller.

Figure 3: Centrifugal Compressor impeller

Initially, a CMM at Science and Technology Center of Excellence (STCE), Ministry of Military Production, is used to individually measure point coordinates on the impeller blades, hub, shroud and compressor diffuser.
However, some complications with collecting point cloud data when using CMM for the impeller blades as will be discussed later which led to the decision to use an optical scanner for the impeller scan.
The optical scanner is a much less cumbersome tool compared to the CMM. Prior to scanning, the part is sprayed with a white, reflective powder coating. A single scan then creates a point cloud of the geometry in view of the component lens. The scanner is re-orientated relative to the model in order to scan all the CAD software. Then, the

resulting point cloud is exported in stl type file to be processed on Siemens NX software to handle the parameterized model of the compressor parts.

3.2 Disassembling Parts Sequence

The disassembly sequence of the JetCat P200-SX centrifugal compressor can be described as follows, see figure 4:

- Disassemble thermocouple extending along the engine from the inlet casing up to the exhaust gas temperature sensor at nozzle exit.
- Remove pink casing covering electronic circuitry.
- All electronics related with Engine Control Unit (ECU) is taken out except the line connecting the starter and the circuit.
- Starter assembly can be pulled out with the rest of the electronic circuits.
- Disassemble shroud casing covering the centrifugal compressor.
- Take off the fuel supply system and housing body structure.
- Both the impeller and the diffusers can easily be reached after this stage.

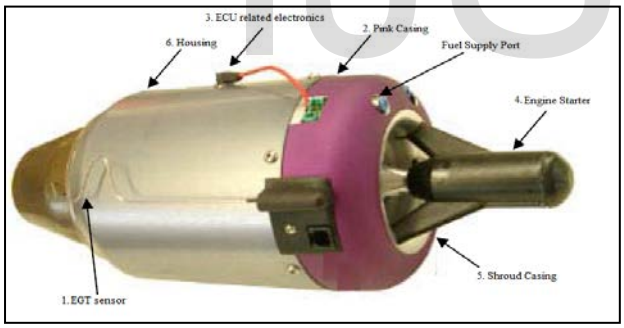

Figure 4: JetCat P200-SX Disassemble Sequence

3.2 Geometry Scanning

A Coordinate Measuring Machine (or CMM) was used to individually measure point coordinates on the centrifugal compressor components (impeller, vaneless diffuser, radial vanned diffuser and outlet elbow with axial vanned diffuser) as in figure 5. The small size of the impeller made it so difficult to obtain an accurate measurement because the impeller features were so small, relative to the scanning sensor, the sensor had to be re-orientated several times to allow access to all areas of the impeller while avoiding contact between other parts of CMM and impeller. The sensor longitudinal axis also had to be as normal to the measured surface as possible. The constant re- orientation of the probe caused the resulting point cloud data to have some inaccuracies. Problem areas included the leading-edge profiles of the main and splitter blades as well as the shape of the blade profiles.

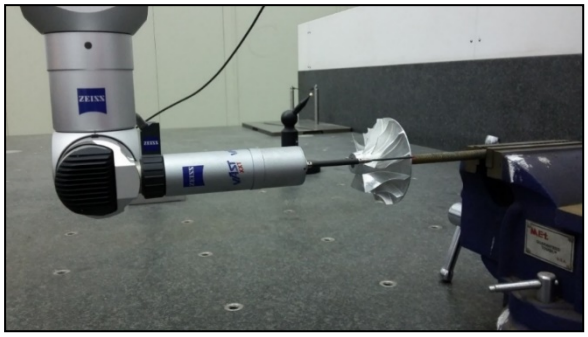

Figure 5: CMM on JetCat P200-SX impeller

To solve this problem an optical scanner is used for the impeller blades and splitters. The optical scanner is a much less cumbersome tool compared to the CMM. Figure 6 shows the optical scanner used on impeller.

Figure 6: LLT 2800-25 3-D Optical Scanner

The following actions have been taken into consideration to get the best results before using the optical scanner:

- To overcome the reflecting of laser line over the shiny surfaces of impeller, the whole compressor is powdered with MET-L-CHEK shown in figure 7.
- The compressor is positioned such that the scanner can reach all the deepest sides of all parts.

Figure 7: MET-L-CHEK Spray Powder

Figure 8 shows the working principle of the LLT 2800-25 optical scanner. The scan sensor operates according to the

principle of optical triangulation (light intersection method).

- A laser line is projected onto the target surface via a linear optical system.
- The diffusely reflected light from the laser line is replicated on a complementary metal-oxide semiconductor (CMOS) array by a high quality optical system and evaluated in two dimensions.

The laser line triangulation corresponds in principle to the triangulation of a laser point. In addition, during the measurement a row of lines are simultaneously illuminated by the laser line. Apart from the distance information (Z axis), the exact position of each point on the laser line (X axis) is also acquired and output by the system.

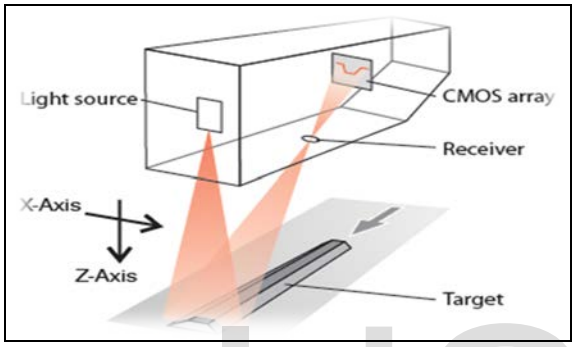

Figure 8: Working Principle of an Optical Scanner

The resulting point cloud in *stl* file from the optical scanner is shown in figure 9.

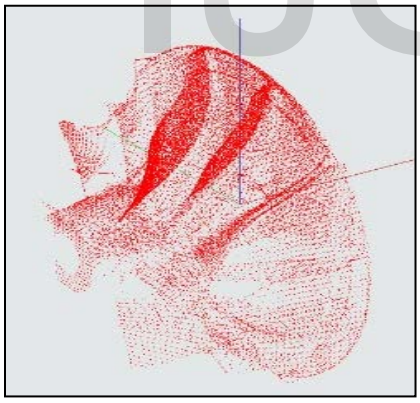

Figure 9: Point cloud resulting from optical scanner

3.2 3-D Geometry Generation

The impellers of a centrifugal compressor are either radial or twisted. Radial impellers are in fact defined in 2-D coordinate space. The solid radial impeller is the extruded version of a 2-D sketch. On the contrary, twisted impellers are fully 3-D shapes. The radial impellers are defined in (r, θ) plane while twisted impellers are defined in (r, z, θ) space. As a result, twisted impellers are more difficult to model and include many parameters for the definition of the full geometry. In order to have a parameterized model of the centrifugal compressor, the scanner output model is processed in Siemens NX software environment. Two splines are created on hub and shroud camber lines and by creating a ruled surface through these splines, the 3-D impeller geometry is obtained as shown in figure 10.

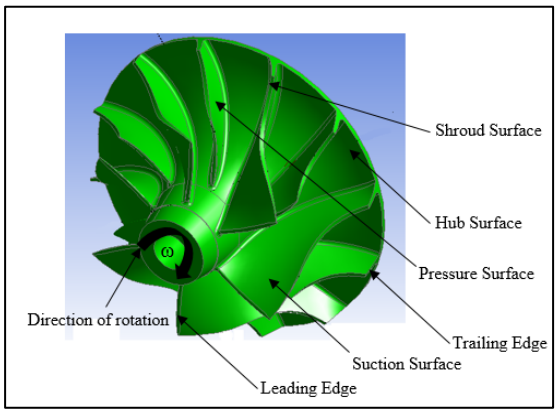

Figure 10: Impeller in IGES Format

Some important terminologies used in the geometric modelling process of the centrifugal compressor are given in figure 11 [5].

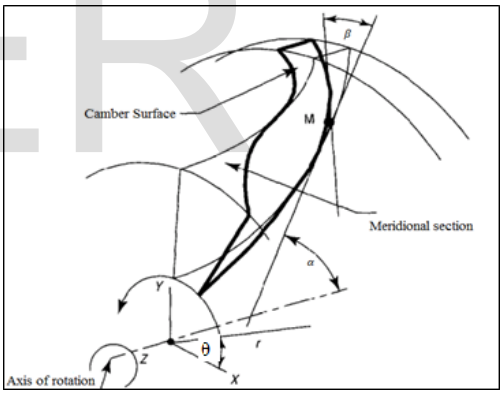

Figure 11: Coordinates, meridional section and the camber

The definitions for terms illustrated in figure 11 are given in Table 2 [5].

Table 2: Terms and Definitions

Term	Definition
Meridional Plane	2-D hub and shroud curves. It forms the mean-line of the blade profile.
Camber Line	3-D curves formed by applying blade angle distribution over 2-D hub and shroud curves. It forms the mean-line of the blade profile.

Blade Angle, β	β angle representing the amount of turn that a blade makes with respect to axial direction
Theta Angle, θ	θ angle that a blade covers which is measured from the beginning of the blade up to the end
Leading Edge	The edge of the blades at the inlet which is the first boundary to force the fluid flow.
Tailing Edge	The edge of the blades at the exit.
Splitter	Additional, smaller blades placed circumferentially between the main blades.
Cut-off Ratio	Splitter hub or shroud curve meridional lengths divided by main blade hub or shroud meridional lengths respectively.
Suction Surface	The convex surface of the blade along which the pressure is lower.
Pressure Surface	The concave surface of the blade along which the pressures are higher.

Using the same procedure with the data obtained from the CMM, the 3-D model of the vaneless and vanned diffuser can be generated as shown in figures 12 and 13.

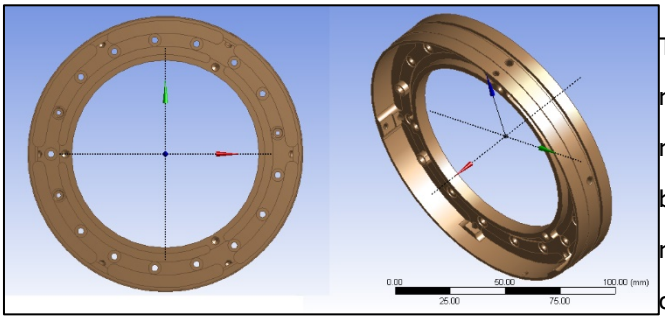

Figure 12: Vaneless diffuser in IGES format

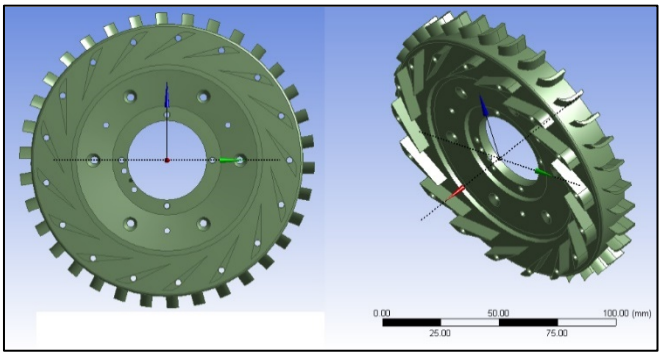

Figure 13: Vanned diffuser in IGES format

By assembling the models obtained the full 3-D model of the JetCat P200sx compressor can be generated as shown in figure 14.

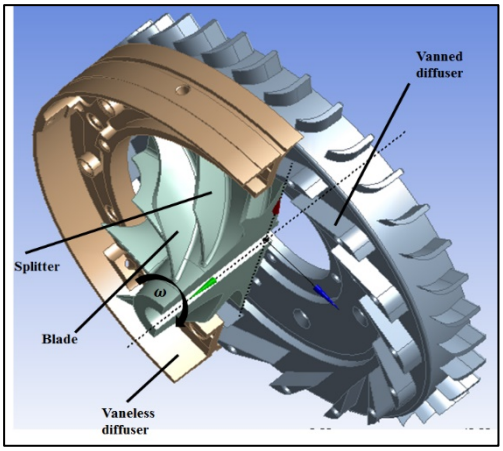

Figure 14: JetCat P200sx centrifugal compressor in IGES format

The cut-off ratio which defines the length of splitter at the hub and shroud are measured in the meridional view as in figure 15.

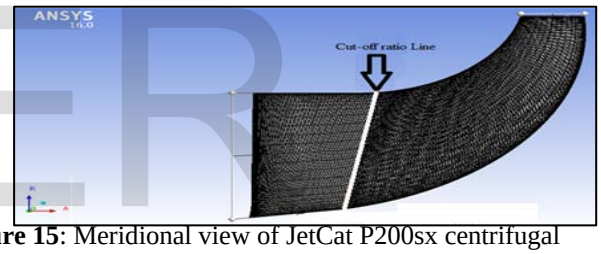

Figure 15: Meridional view of JetCat P200sx centrifugal compressor

The blade angles β, θ and the thickness of the blade are measured by using measurement tools of the 3-D modelling software Siemens NX. Splitters use the main blade's angular and thickness distribution. Therefore, the main blade is created initially and then splitter models are obtained by applying the related cut-off ratios on the main blade.

The blade angles on hub and shroud at the exit are also measured by NX and found to be 5° and 10° respectively. Analyzing the original geometry model shows that the blades are of "backswept" type. Namely, the relative velocity of the fluid exiting the blades makes an angle with the surface normal.

The main parameters to form a parametric centrifugal compressor model and their values for the original case is

summarized in Table 3.

Table 3: Parametric centrifugal compressor model and values

Parameter	Symbol	Value
Blade inlet angle at hub	*βih*	45°
Blade exit angle at hub	*βeh*	5°
Blade inlet angle at shroud	*βis*	69°
Blade exit angle at shroud	*βes*	10°
Inlet theta angle at shroud	*θih*	0°
Exit theta angle at hub	*θeh*	52°
Splitter cut-off ratio at hub	*CORh*	0.8
Splitter cut-off ratio at shroud	*CORs*	0.6
Thickness	*t*	1 mm

3. AEROTHERMODYNAMIC DESIGN

The obtained basic parameters of the compressor from the thermal cycle: total pressure ratio, total adiabatic efficiency and mass flow together with the scanned dimensions are used to validate the reverse aerothermodynamic design procedure using the mean streamline approximation [6]. The main dimensions of the compressor are shown in Table 4. These dimensions are measured from the obtained 3-D model and to be used as a guideline for the reverse design process.

Table 4: Main Dimensions of Compressor (m)

D_{1e}	Compressor inlet diameter at shroud	0.0605
D_{1i}	Compressor inlet diameter at hub	0.0218
D_2	Diameter of impeller exit	0.084
D_3	External diameter of bladeless diffuser	0.0885
D_4	External diameter of bladed diffuser	0.120
D_{5-1}	Compressor exit diameters shroud	0.130
D_{5-2}	Compressor exit diameters at hub	0.1163

In turbomachinery, a velocity triangle is a triangle representing the various components of velocities of the working fluid in a turbomachine. The velocity triangles at impeller blade inlet and outlet are shown in figures (16) and (17) [7].

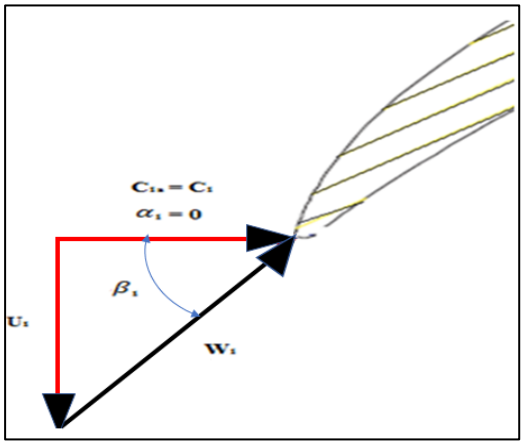

Figure 16: Velocity triangle at Impeller Blade inlet

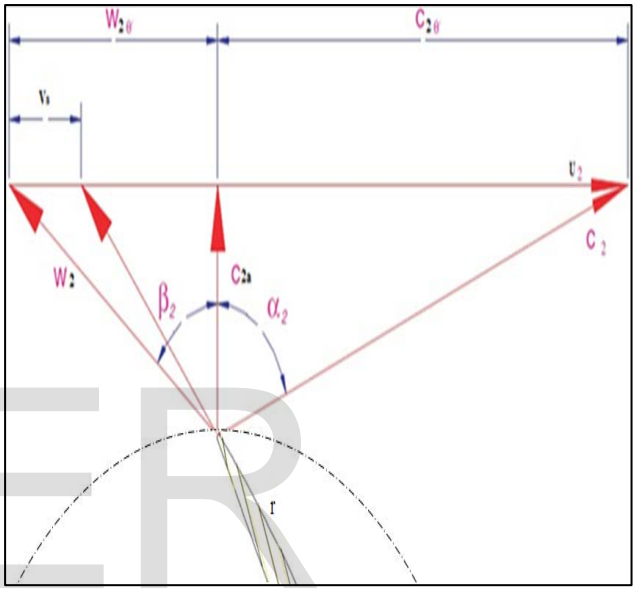

Figure 17: Velocity triangle at impeller blade outlet

3.2 Engine's Thermal Cycle

A complete thermodynamic cycle analysis of the engine at standard conditions is simulated using MATLAB. Some of the specifications of the engine's components and their performance maps are not provided by the manufacturer, therefore in order to solve the thermodynamic cycle at design conditions, an iterative process is implemented using the engines' known parameters (Thrust, air flow rate and EGT) until convergence is reached. The compressor's total adiabatic efficiency (η_{ct}) is estimated to satisfy the engine rated thrust reaching a value of 72.48%.

Air is assumed at standard conditions of 288° K and 101325 Pa at the inlet of the engine. Its specific heat capacity at constant pressure (C_p) and specific heat ratio (γ) are assumed constants, and equal to 1004.5 J/kg.K

and 1.4, respectively [6], [8].

The final main engine thermal cycle parameters (π_{Ct}, T_{3t}) and main engine parameters (F_s, C_s) are given in Table 5 which coincides well with the manufacture data.

Table 5: Main cycle and engine parameters of JetCat P200-SX

Parameter	Cycle Parameters		Engine Parameters	
	π_{ct}	T_{3t} [K]	F_s [N/kg/s]	C_s [kg_f/N.h]
Turbojet Engine JetCat P200-SX Thermal cycle	3.72	1187	511.215	0.151
Manufacture data	3.7	-	511.11	0.1523

3.2 Impeller Design

The mean streamline approximation concept is used for impeller design, as result the meridional plane is obtained. The mean streamline approximation uses the continuity, energy and momentum equations together with some empirical relations based on experience and scanned measuring dimensions. The used basic equations are:

Continuity equation:

$$m = \rho_{1m} A_1 C_{1a} = C_{2r} \rho_2 \pi D_2 b_2 \tau_L \quad (1)$$

Relation for static and stagnation temperature and pressure:

$$T_t = T + \frac{C^2}{2 C_p}, P = P_t(\frac{T}{T_t})^{\frac{\gamma}{\gamma-1}} \quad (2)$$

Momentum equation:

$$l_{ec} = (\mu + \alpha_D) u_2^2 \quad (3)$$

Energy equation:

$$l_{ec} = c_p(T_{2t} - T_{1t}) \quad (4)$$

Efficiency definition:

$$\eta_{Ct} = \frac{l_{adt}}{l_{ec}} = \frac{c_p T_{1t} (\pi_{ct}^{\frac{\gamma-1}{\gamma}} - 1)}{l_{ec}} \quad (5)$$

Since the diameter at impeller exit (D_2) is known from the scanned model, then the Circumferential velocity at impeller exit can be calculated from the previous equation in the following form, $(U_2 = 450{:}\,490)$, [m/s]:

$$U_2 = \frac{\pi n D_2}{60} \quad (6)$$
$$U_2 = 492.6 \text{ [m/s]}$$

Specific Adiabatic work:

$$l_{adt} = c_p T_{1t} \left[(\pi_{ct})^{\frac{\gamma-1}{\gamma}} - 1\right] \quad (7)$$
$$l_{adt} = 133581.3178 \text{ [J/kg]}$$

In this case of study an axial flow entry is presented, $C_{1u} = 0$

To prevent backward flow:

$$(0.16 - 0.22) < \frac{C_{2r}}{U_2} = (0.25 - 0.35) \quad (8)$$

Where:

C_{2r} Radial velocity at impeller exit [m/s]

Select, $C_{2r} = 0.339\, U_2 = C_{1a}$

Nominal axial velocity at impeller entry:

$$C_{1a} = (100\text{-}160) \text{ up to } 180 \text{ [m/s]} \quad (9)$$

The estimated axial velocity satisfying the real impeller inlet area is:

$$C_{1a} = 167.064 \text{ [m/s]}$$

Mean velocity at impeller entry:

$$C_{1m} = \sqrt{C_{1a}^2 + C_{1um}^2}, C_{1um} = 0 \quad (10)$$

Where the inlet area basic dimensions are:

$$D_{1i} = 0.0218 \text{ [m]}, D_{1e} = 0.0605 \text{ [m]}, v_1 = \frac{D_{1i}}{D_{1e}} = 0.36033$$
$$, D_{1m} = 0.04115 \text{ [m]}$$

Diameter of impeller exist, [m]:

$$D_2 = (1.38 - 2.2) D_{1e} \quad (11)$$

The real $D_2 = 0.084$ [m], for which $\frac{D_2}{D_{1e}} = 1.38843$

Kazandzan Slip coefficient:

$$\bar{\mu} = \frac{1}{\left(1 + \frac{2\pi}{3z}\left(\frac{1}{1-\left(\frac{D_{1m}}{D_2}\right)^2}\right)\right)} \quad (12)$$

First law of thermodynamic is used for determination of polotropic exponent n_1 of compression process in impeller:

$$\frac{n_1}{n_1 - 1} = \frac{\gamma}{\gamma - 1} - \frac{\sum l_r}{R\,(T_2 - T_1)} = x \xrightarrow{yields} n_1 = \frac{x}{x-1} = 1.5237 \quad (13)$$

$$\sum l_r = l_{r1} + l_{r2} + l_{rd} \quad (14)$$

Where:

$\sum l_r$ Sum of total losses in impeller, [J/kg], given by:

- Losses due to change of flow direction from axial to radial, [J/kg]:

$$l_{r1} = \xi_1 \frac{w_{1m}^2}{2} \quad (15)$$

Where:

ξ_1 Friction work coefficient, $\xi_1 = (0.1 : 0.2)$

Select, $\xi_1 = 0.2$

- Losses in Impeller, [J/kg]:

$$l_{r2} = \xi_2 \frac{C_{2r}^2}{2} \quad (16)$$

Where:

ξ_2 Friction work coefficient, $\xi_2 = (0.1 : 0.2)$

Select, $\xi_2 = 0.1$

- Disc friction losses, $\alpha_D = (0.06 : 0.08)$,[J/kg]:

$$l_{rd} = \alpha_D\, U_2^2 \quad (17)$$

The solution of all mentioned equations is done through developed MATLAB code. As result the following basic geometrical and thermodynamic parameters of impeller are calculated and shown in Table [6].

Table 6: Basic geometrical and thermodynamic parameters of impeller

Circumferential velocity at impeller exit	$U_2 = 450 : 490$	492.6	[m/s]
Radial velocity at impeller exit	$C_{2r} = 0.339 U_2$	167.064	[m/s]
Optimum axial velocity at impeller entry	$C_{1a} = C_{2r}$, (100-160) up to 180	167.064	[m/s]
Static Temperature at impeller entry	T_{1m}	274.257	[K]
Static pressure at impeller entry	P_{1m}	84755.23	[Pa]
Hub - Tip ratio at compressor inlet	v_1 =0.3:0.6	0.36033	[ ]
The external diameter at impeller entry	D_{1e}	0.0605	[m]
The internal diameter at impeller entry	D_{1i}	0.0218	[m]
Diameter of impeller exit	$D_2 = (1.38 - 2.2) D_{1e}$	0.084	[m]
Circumferential velocity at impeller entry at external diameter	u_{1e}	354.790	[m/s]
Static temperature at impeller entry at external diameter	T_{1e}	274.257	[K]
Relative velocity at impeller entry at external diameter	w_{1e}	392.156	[m/s]
blade width	b_2	0.007	[m]
Total temperature at impeller exit	T_{2t}	471.63	[K]
Static	T_2	400.59	[K]

temperature at impeller exit			

Checking of Mach number at Impeller entry at external diameter gives:

$$Mw_{1e} = \frac{w_{1e}}{\sqrt{\gamma R T_{1e}}} = 1.1813 \quad (18)$$

Which satisfies the constrains given by:

$$Mw_{1e} < (0.8: 1.2)$$

Checking:

$$\frac{b_2}{D_2} = (0.04 - 0.08) = 0.0833 \quad (19)$$

3.2 Bladeless Diffuser Design

The same basic equations are applied for the solution of flow field in the bladeless diffuser in addition to the corresponding empirical relations:

Width of Bladeless Diffuser Interface, [mm]:

$$b_{2d} = b_2 + \Delta 1 = 7.6\ [mm] \text{ (real blade thickness)} \quad (20)$$
$$\Delta 1 = (0.6 - 0.8)\ \text{mm}, \text{select}\ \Delta 1 = 0.6$$

External diameter Of Bladeless Diffuser, [m]:

$$D_3 = (1.05 - 1.15) D_2, \quad (21)$$
$$\text{select}\ D_3 = 1.054\ D_2 = 0.08854\ [\text{m}]$$

(real measured value)

Outer flow angle from the Bladeless Diffuser, [Degree]:

$$\alpha_3 = \text{atan}[\tan \alpha_{2d} + \frac{\xi_r}{b_3}(r_3 - r_2)] \quad (22)$$
$$\alpha_3 = 23.656°$$

Where:

ξ_r Friction coefficient, $\xi_r = (0.75: 1)10^{-2}$

Select, $\xi_r = 0.01$

Friction work in Bladeless Diffuser, [J/kg]:

$$l_r = \frac{\xi_r}{4 b_3} \frac{C_{2d}^2 - C_3^2}{\sin \alpha_m} (r_3 - r_2) \quad (23)$$
$$l_r = 90.886$$

The solution of all mentioned equations together with geometrical constrains given by the scanned values of real compressor parts is done by MATLAB code, where the folowing basic parameters of the bladeless diffuser are given in Table 7.

Table 7: Basic parameters of bladeless diffuser

Total temperature at impeller exit (Energy Equation)	$T_{2t} = T_{3c} = T_{4c}$	471.63	[K]
Width of Bladeless Diffuser Outlet	$b_3 = b_{2d}$	0.0076	[m]
Density at Bladeless Diffuser exit	ρ_3	2.622	[kg/m^3]
Outlet radial velocity from the Bladeless Diffuser	C_{3r}	118.214	[m/s]
Outlet Absolute velocity from the Bladeless Diffuser	C_3	294.615	[m/s]
Static temperature at bladeless diffuser	T_3	428.42	[K]
Static pressure at bladeless diffuser	P_3	32240.43	[Pa]
Total pressure at bladeless diffuser	P_{3t}	451277.77	[Pa]
The mean polotropic exponent of compression process in Bladeless diffuser	n_2	1.402	[ ]

Checking of mach number at bladless diffuser exit:

$$M_{c3} = \frac{C_3}{\sqrt{R_a\ T_3 \gamma_a}} = 0.71$$

Which satisfies the constrains given by:

$$M_{c3} \leq (0.85 - 0.95)$$

3.2 Bladed Diffuser Design

Similar procedure is applied for the bladed diffuser design, with selecting circular meanline for the diffuser blade and selecting and calculating the following parameters:

Incidence angle, [Degree]:

$$i = \pm 1 \quad (24)$$

Geometric Angle, [Degree]:

$$\alpha_{3k} = \alpha_3 + i = 24.656 \quad (25)$$

Width of Bladed Diffuser, [m]:

$$b_4 = b_3 \quad (26)$$

Flow angle, [Degree]:

$$\alpha_4 = \alpha_3 + (12 - 20^o) = 35.656 \quad (27)$$

Geometric Angle, [Degree]:

$$\alpha_{4k} = \alpha_4 + (2 - 4^o) = 37.656 \quad (28)$$

The external diameter of bladed diffuser, [m]:

$$D_4 = (1.25 - 1.35)D_3 = 1.35532\ D_3 = 0.12 \quad (29)$$

Friction work in Bladeless Diffuser [J/kg]:

$$l_r = \xi_{diff}\ \frac{C_3^2 - C_4^2}{2} = 5064.344 \quad (30)$$

Where:

ξ_{diff} Friction work coefficient, $\xi_{diff} = (0.1: 0.2)$, depended upon the angle of divergence of the bladed diffuser, $\theta = 3.0742°$, for which $\xi_{diff} = 0.135$

The following basic parameters for bladed diffuser are given in Table 8.

Table 8: Basic parameters of bladed diffuser

Number of blades of the diffuser	Z_{LD}	17	[ ]
Absolute velocity at bladed diffuser	C_4	113.58	[m/s]
Static temperature at bladed diffuser	T_4	468.95	[K]
The mean polotropic exponent of compression process in Bladed diffuser	n_3	1.493	[ ]
Density at bladed diffuser	ρ_4	3.034	[kg/m³]
The blade thickness	t_d	0.005	[m]

3.2 Outlet Elbow Design

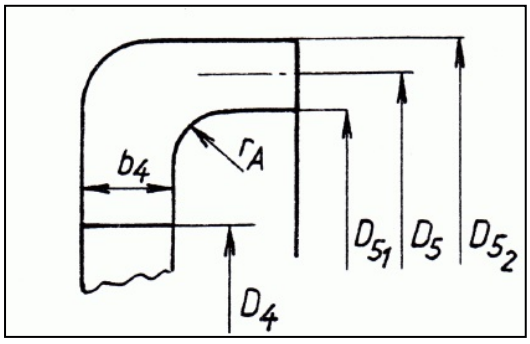

Figure 18: Outlet Elbow Main Dimensions

Outer diameter of outlet elbow, [m]:

$$D_5 = D_4 + 2b_4 \quad (31)$$

Absolute velocity at outlet elbow, [m/s]:

$$C_5 \equiv C_{5a} = (60 - 120\ ) \quad (32)$$

Such velocity is calculated using iteration with MATLAB to satisfy the mass flow rate and real dimensions:

$$C_5 = 61.07\ \ [m/s]$$

The total temperature at outlet elbow, [K]:

$$T_{5c} = T_{2t} \quad (33)$$

Staic temperature at outlet elbow, [K]:

$$T_5 = T_{5c} - \frac{C_5^2}{2C_p} = 469.77 \quad (34)$$

The total outlet pressure from compressor is calculated which gives, [Pa]:

$$P_{5c} = 380259.11$$

Checking:

- Compressor pressure ratio:

$$\pi_{ct}(\text{calculated}) = \frac{P_{5c}}{P_{1t}} = 3.774 \quad (35)$$

- Compressor efficiency:

$$\eta_{ct}(\text{calculated}) = \frac{\pi_{ct}^{\frac{\gamma-1}{\gamma}} - 1}{\frac{T_{2t}}{T_{1t}} - 1} = 0.724 \quad (36)$$

4. CFD SIMULATION

To vaildate the results obtained by the develped methodology a CFD software, ANSYS-CFX, is used to calculate the compressor performance at design point speed.

The mesh of the model is created with ANSYS TurboGrid, which automates the creation of high quality hexahedral meshes desired for blade passages in the rotating impeller and the diffuser.

At the compressor model four interfaces are located, the first one is between the intake device and the impeller sub domain, the second one is connecting the impeller and the vaneless diffuser, the third one connects the vaneless diffuser with the radial blade of the vanned diffuser and the last one is located between the radial part of diffuser and the exit sub-domain which contains the axial part of diffuser, see details on figure 19.

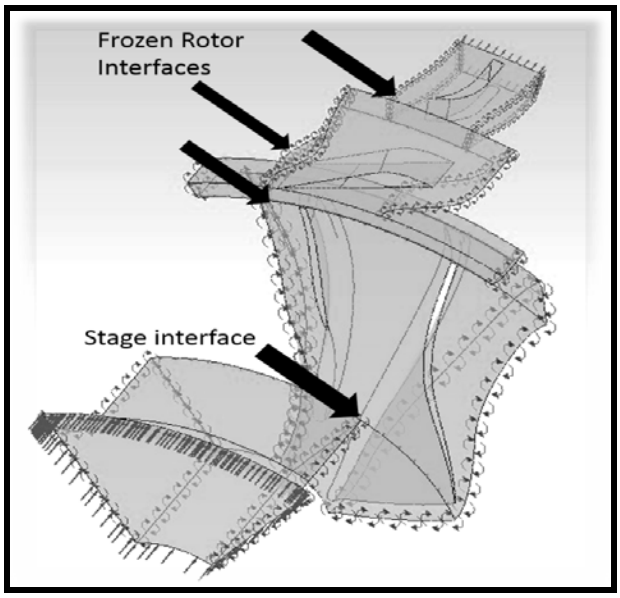

Figure 19: Domain Interfaces in JetCat's Compressor

In this paper, a turbulent single-phase flow is simulated, the fluid is air as idle gas, the reference pressure of 0 Pascal as gauge pressure is selected, the boundary conditions are as follows:

- total pressure at inlet
- total temperature at inlet
- static pressure at outlet
- 5 % turbulence intensity at inlet

A constant physical time step of 1E-4 is used and the mass flow rate $\dot{m}$ is evaluated at the centrifugal compressor exit.

Computations have solved steady and compressible Navier-Stokes equations, joined with k -ε turbulence model.

The obtained results of CFD simulation [9] are as shown in Table 9 compared with the compressor basic parameters used in its reverse aerothermodynamic design.

Table 9: CFD results at Design Point compared with the compressor basic parameters

No.	Quantity calculated	CFD	Compressor basic parameters	Deviation %
1	Pressure ratio (π_{ct})	3.7482	3.774	0.76
2	Total efficiency (η_{ct})	0.7227	0.7248	0.29
3	Mass Flow Rate, [kg/s]	0.45216	0.45	-0.47

5. CONCLUSION

The objective of this work is the reverse design an UAV TJE centrifugal compressor with certain design point and characteristics. The objective is reached by scaning the compressor dimensions and applying the reverse aerothermodynamic design using the mean streamline approximation concept. The analytical analysis of the thermodynamic cycle combined with some empirical formulas of compressor and combustion chamber performance is found suitable for a preliminary analysis of a micro-turbojet engine cycle. The MATLAB code is created keeping in mind different user requirements with regards to compressor basic parameters given by pressure ratio, efficiency and mass flow rate at design point and dimensional constraints.

Finally a CFD simulation is performed to evaluate the used reverse aerothermodynamic design methodology written in MATLAB. The comparison of the obtained results show very good agreement with deviation less than 1%.

6. NOMENCLATURE

Symbol	Description
C_{1a}	optimum axial velocity at impeller entry, [m/s]
C_{1u}	circumferential component of axial velocity at impeller entry, [m/s]
C_1	Absolute velocity at impeller entry, [m/s]
C_2	Absolute velocity at impeller exit, [m/s]
C_{2a}	optimum axial velocity at impeller exit, [m/s]
C_{2u}	circumferential component of axial velocity at impeller exit, [m/s]
$\dot{m}$	Mass Flow rate
U_1	Blade velocity at Impeller entry, [m/s]
U_2	Blade velocity at Impeller exit, [m/s]
W_1	Relative velocity at Impeller entry, [m/s]
W_{1a}	optimum relative velocity at Impeller entry, [m/s]
W_{1u}	circumferential component of relative velocity at impeller entry, [m/s]
W_2	Relative velocity at Impeller exit, [m/s]
W_{2a}	optimum relative velocity at Impeller exit, [m/s]
W_{2u}	circumferential component of relative velocity at impeller exit, [m/s]

7. GREEK LETTERS

α_1	absolute angle at impeller entry, [degree]
α_2	absolute angle at impeller exit, [degree]
β_1	Relative angle at impeller entry, [degree]
β_2	Relative angle at impeller exit, [degree]
η	Efficiency
π_{ct}	Pressure ratio

8. ABBRIVIATIONS

ANSYS	Analysis of Systems
CFD	Computational Fluid Dynamics

IGES	Initial Graphics Exchange Specification
stl	STereoLithography
TJE	Turbo Jet Engine
UAV	Unmanned Aerial vehicle

REFERENCES

[1] Raja, V. and Fernandes, K.J., Reverse Engineering: An Industrial Perspective, London: Springer Science, 2007.

[2] A.Satish, Dr. K.Rambabu, M.Ramji," Centrifugal Pump Impeller Modeling With Reverse Engineering," Engineering College, Eluru, AP, India, 2014.

[3] "JetCAT USA," http://www.jetcatusa.com/

[4] Arda Ceylanoglu, "An Accelerated Aerodynamic Optimization Approach for a Small Turbojet Engine Centrifugal Compressor," Master thesis, The Graduate School of Natural and Applied Sciences of Middle East Technical University, Turkey, 2009.

[5] Bohez, L.J., Pole, K., A Geometric Modeling and Five-Axis Machining Algorithm for Centrifugal Impellers, Journal of Manufacturing Systems, vol. 16 no. 6 (422-436), 1997.

[6] Elzahaby, A. M. Theory of jet engines, Printed lectures: Military technical college, MTC, Egypt, 2013.

[7] Compressors—Handbooks, manuals, I. Hanlon, Paul 2001.

[8] KMOCH, P. Aircraft engine theory calculation exercises I (in Czech). Brno: VAAZ, 1972. 56 p. U-2335/I.

[9] ANSYS-CFX Solver Theory Guide, ANSYS Inc., 2016.

[10] Elzahaby, Mohamed K. Khalil, Hesham E. Khalil, "Theoretical and Experimental Analysis of a Micro Turbojet Engine's Performance", International Journal of Scientific &Engineering Research, Volume 7, Issue 1, January 2016.